Magnetic properties of the multiferroic compounds $Eu_{1-x}Y_xMnO_3$ (x = 0.2 and 0.3)

View the article online for updates and enhancements.

Related content

- A SR study of the ruthenium perovskites $ACu_3Ru_4O_{12}$ with A = Ca, Pr, Nd
  G M Kalvius, O Hartmann, A Günther et al.

- Low temperature incommensurately modulated and noncollinear spin structure inFeCr2S4
  G M Kalvius, A Krimmel, O Hartmann et al.

- SR Measurements of the Magnetism of $Sr_3Fe_2O_7$
  W A MacFarlane, D C Peets, T Buck et al.

Recent citations

- Non-collinear magnetism in multiferroic perovskites
  Eric Bousquet and Andrés Cano

IOP ebooks™

Bringing you innovative digital publishing with leading voices to create your essential collection of books in STEM research.

Start exploring the collection - download the first chapter of every title for free.

Magnetic properties of the multiferroic compounds Eu$_{1-x}$Y$_x$MnO$_3$ ($x=$ 0.2 and 0.3)

G M Kalvius[1], **F J Litterst**[2], **O Hartmann**[3], **R Wäppling**[3], **A Krimmel**[4], **A A Mukhin**[5], **A M Balbashov**[6] **and A Loidl**[4]

[1] Physics Department, Technical University Munich, 85747 Garching, Germany
[2] IPCM, Technical University Braunschweig, 38106 Braunschweig, Germany
[3] Department of Physics and Astronomy, Uppsala University, 75120 Uppsala, Sweden
[4] Experimental Physics V, University of Augsburg, 86159 Augsburg, Germany
[5] General Physics Institute, Russian Academy of Sciences, 119991 Moscow, Russia
[6] Moscow Power Engineering Institute, 105835 Moscow, Russia

E-mail: `kalvius@ph.tum.de`

Abstract. Magnetic properties of multiferroic Eu$_{1-x}$Y$_x$MnO$_3$ with $x=0.2, 0.3$ were studied by μSR and Mössbauer spectroscopy. Both compounds are known to become antiferromagnetic with Mn^{3+} being the only magnetic ion. We find $T_N = 47\pm0.5$ K for $x=0.2$ and 45 ± 0.5 K for $x=0.3$. Below T_N three different magnetic states (AFM-1, AFM-2, AFM-3) are formed. The μSR parameters of the uppermost magnetic state (AFM-1) are alike in both compounds, and compatible with a commensurate modulated collinear spin structure. The magnetic ground state in $x=0.2$ (AFM-3) is shown to be single phase. Its spectral parameters support the proposal of a cone-like spin structure, yet with incommensurate modulation. The ground state for $x=0.3$ is found to have an incommensurate spiral spin structure. ^{151}Eu Mössbauer spectroscopy measured the Eu hyperfine field induced by the Mn^{3+} ions. Its low value (~4 T) means that mixing with higher Eu electronic states is small and that the Mn-Eu exchange coupling is weak (~0.5 K). The various magnetic transitions appear as small irregularities in the temperature dependence of the hyperfine fields. The present results are discussed in terms of different published magnetic phase diagrams of Eu$_{1-x}$Y$_x$MnO$_3$.

1. Introduction

Multiferroics are materials where long-range magnetic and polar order coexist with both order parameters being strongly coupled [1]. The perovskites Eu$_{1-x}$Y$_x$MnO$_3$ show multiferroicity without rare earth magnetism since Eu is in the non-magnetic 3+ state. The only magnetic ion is Mn^{3+} which occupies the B-site. Replacing Eu in part by Y changes the A-site volume (see Fig. 1-a) and with it the multiferroic properties, free from the additional influence of a magnetic rare earth moment. Standard μSR is not suited to explore internal electric fields since the muon has no quadrupole moment. For a small number of cases the magneto-electric coupling has been probed with muons in electric field measurements. The present μSR studies investigate the pure volume effect on the magnetic properties of Mn^{3+} in Eu$_{1-x}$Y$_x$MnO$_3$.

A (x,T) phase diagram establishing the different ordered magnetic and polar states of Eu$_{1-x}$Y$_x$MnO$_3$, obtained from structural, magnetic, dielectric and thermodynamic data by [2] and [3], is shown in Fig. 1-b. Details of the sequence of the magnetic states for the compounds studied are depicted in Fig. 1-c. Slightly later, another study of Eu$_{1-x}$Y$_x$MnO$_3$ using

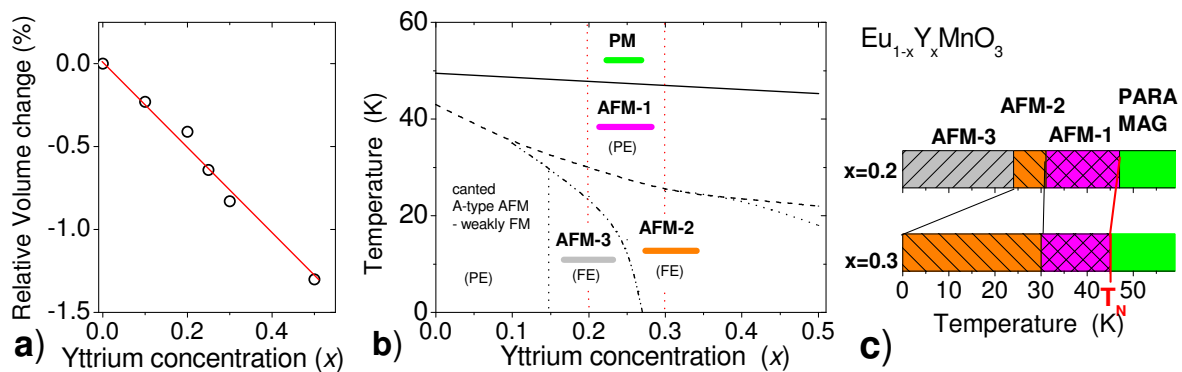**Figure 1.** a) Change of unit cell volume with Y concentration (after [2]). b) Phase diagram of $Eu_{1-x}Y_xMnO_3$ according to [2, 3]. c) The antiferromagnetic states for $x = 0.2$ and 0.3 in detail.

magnetization, dielectric and structural measurements [4] led to an alternate phase diagram where the main difference concerns the $x = 0.2$ compound. The weakly ferromagnetic (canted A-type antiferromagnet) state that is found in [2] as the second magnetic state only for $x \leq 0.1$ is extended to $x \approx 0.27$. In consequence, this state which must be paraelectric on structural arguments, is then the ground state for $Eu_{0.8}Y_{0.2}MnO_3$. The aim of this study is to gain additional information on the magnetic states of $Eu_{0.8}Y_{0.2}MnO_3$ and $Eu_{0.7}Y_{0.3}MnO_3$ from the study of internal fields. We shall discuss in section 6 our findings from μSR and Mössbauer spectroscopy with respect to the results of [2, 3] and [4] as well as additional studies by [5, 6].

2. Experimental
The powder material used was prepared using standard solid state reaction procedures [7]. The samples consisted of non-oriented small single crystalline grains prepared from the the same batch of materials used in [2]. Powder X-ray diffraction revealed single phase material with proper crystallographic structure. For the μSR measurements, the powder was pressed into tablets which were mounted between thin aluminized Mylar foils in the helium gas flow of a variable temperature cryostat. Data were recorded at the 'DOLLY' set-up of the Swiss Muon Source in zero field (ZF) and weak (10 mT) transverse field (TF). The VETO mode was enabled for suppressing the "background signal" from muons stopped outside the sample. Its absence was verified by TF measurements.

3. μSR data for $Eu_{0.8}Y_{0.2}MnO_3$
As depicted in Fig.2-a, the spectra change around 47 K from an oscillatory pattern (in TF) or a simple exponential decay (in ZF), both typical for the paramagnetic state, to the characteristic pattern for polycrystalline long-range ordered (LRO) magnets given by:

$$A_{LRO}(t) = A_0[(2/3)\exp(-\lambda_{tr}\,t)\cos(2\pi\nu_\mu\,t + \varphi) + (1/3)\exp(-\lambda_{lg}\,t)] \quad (1)$$

with $\nu_\mu = \gamma_\mu B_\mu/2\pi$ where B_μ is the mean field at the muon site, and γ_μ the muon gyromagnetic ratio. The transverse relaxation rate is a measure of the static field distribution width ($\Delta B_\mu = \lambda_{tr}/\gamma_\mu$), while the longitudinal rate λ_{lg} gives the fluctuation rate of the ordered atomic moments (here the Mn^{3+} moments) with $\lambda_{lg} \propto 1/\tau_{Mn}$. Eq. (1) is strictly valid only in ZF, but also holds for weak TF ($B_{TF} \leq B_\mu$). Between 47 K and 50 K the μSR spectra consist of the sum of the paramagnetic and the LRO signals (see spectrum at 47.5 K in Fig.2-a). This means that the sample is a heterogeneous mixture of paramagnetic and LRO fractions. The temperature dependence of the paramagnetic fraction is shown in Fig.2-b. The transition into the LRO state
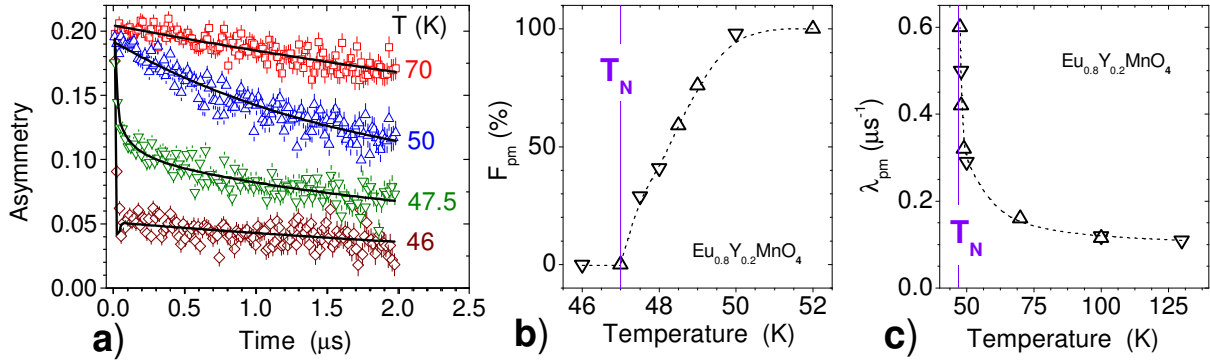
Figure 2. a) ZF spectra around T_N. The lines are fits discussed in text. Temperature dependences of b) the paramagnetic fraction F_{pm} and c) the paramagnetic relaxation rate λ_{pm}. $\triangledown$ =ZF data, $\triangle$ = TF data. The broken lines are guides to the eye.

is spread out over $\sim 3\,$K. Taking as Néel temperature the first appearance of the LRO pattern gives $T_N = 47 \pm 0.5\,$K in agreement with bulk magnetic data [2]. The paramagnetic relaxation rate exhibits the typical sharp rise on approach to a second order phase transition (Fig.2-c).

Fig. 3-a displays the early time parts of typical ZF spectra below T_N, and Fig. 3-b the temperature dependences of the magnetic parameters. The spectra at 47, 46 and 43 K, characteristic for the AFM-1 state, can be fitted well using Eq. (1). They are fully consistent with a commensurate modulated collinear spin structure. The spin modulation causes a large field distribution width $\Delta B_\mu / B_\mu(0) \sim 1$, provided the modulation wavelength is not too short. A short wavelength would result in a structured field distribution that is not observed. It cannot be excluded that small distortions of the collinear spin structure on a local scale also contribute to ΔB_μ. At 27 K we obtain a spectrum similar to those recorded at 20 K (not shown) and 10 K (i.e., in AFM-3). The μSR data indicate a direct transition from the AFM-1 state into the AFM-3 ground state.

Fitting the spectra of the AFM-3 state in the same manner as the AFM-1 spectra lead to unreasonably large values of the phase φ given in Eq. (1). This feature is indicative for the need
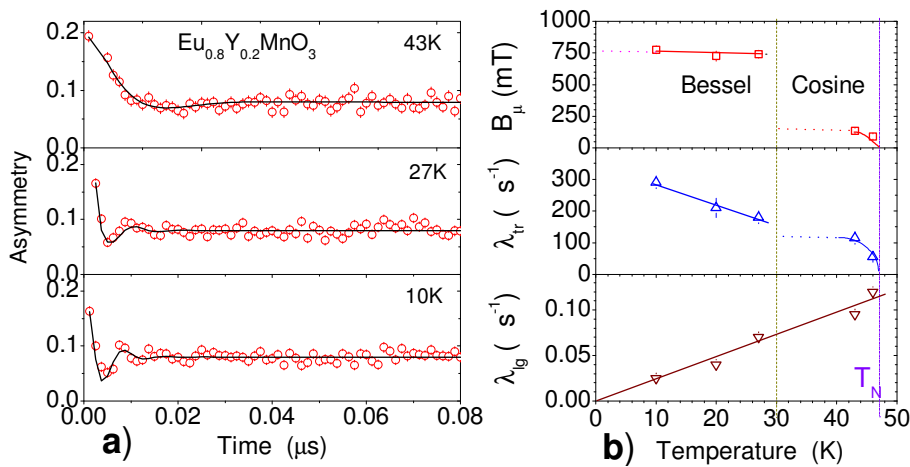

Figure 3. a): Selected ZF spectra of $Eu_{0.8}Y_{0.2}MnO_3$ at different temperatures. The lines are fits discussed in text. b): Temperature dependences of the local field B_μ, the transverse (λ_{tr}) and longitudinal (λ_{lg}) relaxation rates. The lines trough the data points are guides to the eye.

to replace the cosine function by the first order Bessel function J_0 [8]. At least for simple cases like a sinusoidally modulated spin structure, it has been shown [8, 9] that the Bessel function is the result of incommensurability of the modulation. μSR is not a reciprocal space probe like neutron diffraction and hence gives no direct information of the spatial arrangements in LRO spin structures. But quite generally, the appearance of of Bessel oscillations in the μSR spectra can be taken as an indication for incommensurate spin modulation (see examples in [9]). Neutron data on the spin structure are not reported. The Bessel function takes care of the field distribution caused by the incommensurate spin modulation [8]. The frequency of Bessel oscillations is given by the maximal field of this field distribution, in contrast to the cosine oscillations where ν_μ is given by the mean field. For clarity we use in the figures B_μ for both situations. B_μ increases sharply at the 30 K transition. The transverse relaxation rate is still large in AFM-3 ground state. Since the Bessel function takes care of the field distribution caused by the incommensurate spin modulation, the substantial distribution width given by $\lambda_{\rm tr}$ points to some additional random local disturbances in the AFM-3 spin structure. The spin fluctuations reflected by $\lambda_{\rm lg}$ show the expected move toward the static limit for $T \to 0$. They are not affected by the changes in spin structure, an observation also made in other magnetic compounds (see, for example [9]). It indicates that the slow electronic moment fluctuations seen uniquely by μSR do not exhibit critical behavior at the transit to a different spin arrangement.

4. μSR data for $\mathbf{Eu_{0.7}Y_{0.3}MnO_3}$
Using the same procedures as those employed for $x = 0.2$ leads to $T_{\rm N} = 45 \pm 0.5$ K. Again one observes a small spread over ~ 3 K of the transition regime and the strong rise in paramagnetic relaxation rate (from $0.15\,\mu{\rm s}^{-1}$ at 60K to $1.5\,\mu{\rm s}^{-1}$ at 46K) on approach to $T_{\rm N}$, confirming here as well the second order nature of the transition at $T_{\rm N}$.
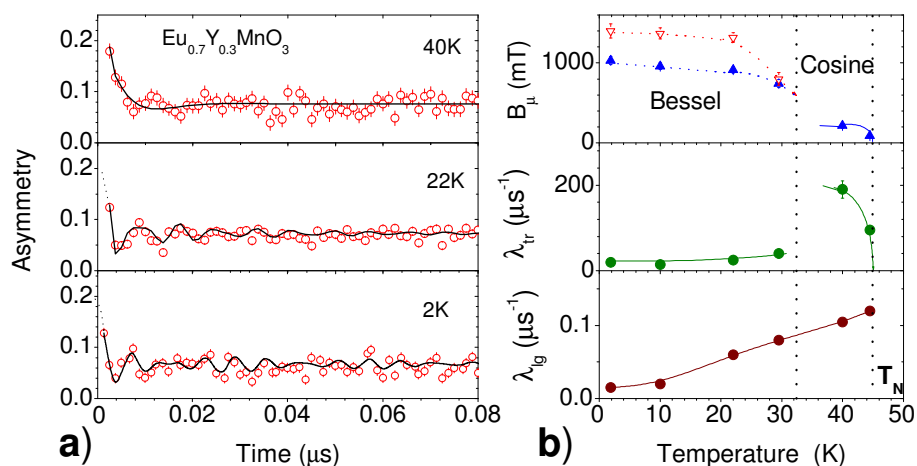

Figure 4. a): Selected ZF spectra of $\mathrm{Eu_{0.7}Y_{0.3}MnO_3}$ at different temperatures. The lines are fits discussed in text. b): Temperature dependences of the local field B_μ, the transverse ($\lambda_{\rm tr}$) and longitudinal ($\lambda_{\rm lg}$) relaxation rates. The lines through the data points are guides to the eye.

The early time parts of selected ZF spectra taken below $T_{\rm N}$ is presented in Fig. 4-a, and the temperature dependences of the magnetic parameters in Fig. 4-b. Spectra within the AFM-1 regime (e.g., at 40 K) were successfully treated in the same manner as previously for the $x = 0.2$ material, showing that the characteristics of the AFM-1 state are the same in both compounds. Fits of the spectra in the AFM-2 state (taken at 30, 22, and 2 K) reveal a two frequency Bessel oscillatory pattern. At 30 K the two frequency requirement is marginal, but
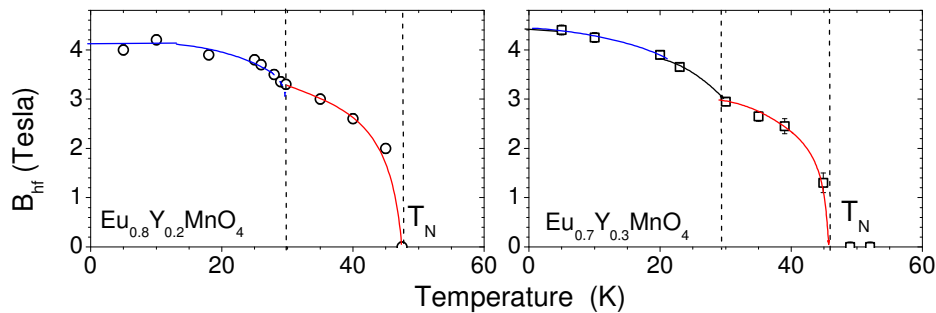
Figure 5. The magnetic field at the ^{151}Eu nucleus (B_{hf}) in $Eu_{0.8}Y_{0.2}MnO_3$ and $Eu_{0.7}Y_{0.3}MnO_3$ versus temperature. The solid lines indicate the extrapolation of B_{hf} to $T \to 0$.

it becomes distinctive at lower temperatures. Since the paramagnetic spectra confirm a single interstitial muon stopping site, the two frequencies must arise from the field distribution of the LRO spin arrangement. It reflects, according to [10], an incommensurate spiral antiferromagnetic structure. We have previously observed in $FeCr_2S_4$ [11] a similar type of spectra and interpreted them the same way. Present in $Eu_{0.7}Y_{0.3}MnO_3$ is also the large jump in B_μ at the transition point and the continuous reduction of λ_{lg} with cooling. In contrast, λ_{tr} is very small meaning the spiral structure is not modulated and well developed on short-range and long-range scales.

5. Mössbauer data

Only a brief summary is presented, more details will be found in a forthcoming publication [13]. The 21 keV resonance of ^{151}Eu was used. Technical features and typical applications of this resonance can be found in [14]. The parameter of concern is the hyperfine field B_{hf} at the Eu nucleus. In standard Mössbauer studies (e.g., ^{57}Fe) it is generated by an unfilled electron shell in the resonant ion. Here, in the resonant ion (Eu^{3+}) all electron orbits are closed and B_{hf} originates from the interaction with the moment on neighboring Mn^{3+} ions, somewhat in analogy to B_μ. Yet, the information contained in B_{hf} is different: (a) The Eu nucleus as the probe is fixed onto a regular lattice site, while the muon sits on an (unknown) interstitial site. (b) B_{hf} is not the raw field of the Mn^{3+} moments at the Eu lattice site. Rather, the field from Mn moments polarizes the Eu electron shell and the field at the nucleus is amplified by this shell distortion and thus enhanced. (c) The coupling between the muon and the Mn field is predominantly dipolar and hence highly sensitive to the geometrical arrangement of the Mn moments. Due to the dominant enhancement by the polarized electron shell, this is not the case for B_{hf}. (d) The ^{151}Eu nucleus has a sizable quadrupole moment and responds also to electrical interactions. Since the magnetic coupling is dominant, and due to the limited resolution resulting from the low size of B_{hf}, the quadrupolar interaction was neglected in first approximation.

B_{hf} versus temperature is plotted in Fig. 5. The slightly higher field in the AFM-1 state of $x = 0.3$ is confirmed. Most noticeable is the much smaller increase of $B_{hf}(0)$ between the AFM-1 state and the magnetic ground states (AFM-3 or AFM-2) when compared to B_μ. This confirms that the large jump in B_μ arises from a change in spin arrangement, rather than from a change in Mn moment. The size of $B_{hf}(T \to 0)$ is only $\sim$4 T, a rather small value compared to $B_{hf}(0)$ produced by an open electron shell in Eu (typically around 30 T [14]). Even for an induced field the size is low which indicates that the distortion of the Eu shell, i.e. the mixing of the non-magnetic ground state with magnetic higher crystalline electric field electronic states, is small and points furthermore to a weak Mn-Eu exchange coupling, estimated to be $\sim$0.5 K.

6. Discussion

We now discuss the results of our μSR and Mössbauer studies on the different magnetic states in $Eu_{0.8}Y_{0.2}MnO_3$ and $Eu_{0.7}Y_{0.3}MnO_3$ in the light of existing bulk magnetic data.

a) The Néel temperatures derived agree well with [2] and confirm their slight decrease with increasing x. The μSR spectra show the coexistence of paramagnetic and antiferromagnetic fractions over a range of $3\,K$ around T_N and confirm further the second order nature of the transition at T_N.

b) The spin structure in the uppermost magnetic state (AFM-1) is similar for $x = 0.2$ and 0.3. The μSR spectra are consistent with a commensurate modulated collinear spin arrangement, as proposed in [2, 4]. The observed wide distribution of the local field requires a not too short modulation wave length (see also [4]). The saturation internal field $B_\mu(T \to 0)$ is somewhat larger in $x = 0.3$ than in $x = 0.2$ as the result of the reduced unit cell volume.

c) The μSR results for the magnetic states following the AFM-1 state on reduced temperature (AFM-2, AFM-3) are characteristic for incommensurate spin structures. The question of incommensurate structures in the ferroelectric ground states had remained open on the basis of bulk measurements [2]. It is, however, not decisive with respect to the multiferroic properties. A sudden rise of B_μ occurs when crossing the lower AFM-1 phase boundary. The corresponding Mössbauer data show that the magnitude of the ordered Mn^{3+} moment does not change much, if at all. The sudden increase of B_μ then reflects a substantial change in spin arrangement.

d) The μSR spectral features of the ground state in $x = 0.3$ (AFM-2) point toward a well developed incommensurate antiferromagnetic spiral structure, in accordance with earlier suggestions on the basis of the ferroelectric properties (see, for example [12]).

e) The μSR data for $x = 0.2$ show that the magnetic ground state (AFM-3) follows directly the AFM-1 state without going through an intermediate phase (AFM-2).

f) As mentioned already in section 1, the nature of the magnetic ground state for $x = 0.2$ is controversial. In [2] the $Eu_{0.8}Y_{0.2}MnO_3$ material shows definitely ferroelectric polarization. The same result is also reported in [5, 6]. It completely contradicts the canted A-type AFM structure claimed by [4] as the $x = 0.2$ ground state, since that state cannot support ferroelectricity on structural grounds. Indeed it is listed as a paraelectric state in the phase diagram of [4]. Two scenarios have been suggested to remedy the situation: (1) The $x = 0.2$ material is heterogeneous having undergone phase separation. It consists of a weakly ferromagnetic fraction having the canted A-type AFM spin structure established for $x \leq 0.1$ and a non-ferromagnetic fraction featuring the antiferromagnetic spin structure of the $x = 0.3$ magnetic ground state. This approach is discussed, in particular, in [6] and [4]. (2) The formation of a new weakly ferromagnetic AFM phase having a spin structure which breaks inversion symmetry. This approach is presented in [2] with the proposal of a non collinear probably cone-like AFM spin structure. A basically similar approach is given in [5].

The μSR data definitely exclude a two phase heterogeneous material. If two fractions with substantially different spin structures would exist, the spectrum should consist of a superposition of two different signals, similar to the coexistence of a paramagnetic and a antiferromagnetic phase around T_N (see Fig. 2-a). The rather involved spectrum of AFM-2 would lead to a very complex sum spectrum. This is not the case. The spectrum can well be fitted by a single μSR signal. Furthermore, a ground state having the canted A-type AFM structure not only contradicts the electric polarization data, but the μSR spectrum as well, which should consist of a simple cosine oscillation and not the Bessel oscillation observed. On the other hand, a non-collinear cone-like incommensurately modulated AFM structure is fully supported by μSR.

in part by the Deutsche Forschungsgememeinschaft (DFG) via the Transregional Collaborative Research Center TRR80 (Augsburg, Munich, Stuttgart)

References

[1] Khomski D I 2006 *J. Magn. Magn. Mat.* **306** 1
[2] Hemberger J *et al.* 2007 *Phys. Rev.* B**75** 035118
[3] Noda K *et al.* 2006 *J. Appl. Phys.* **99** 08S905
[4] Yamasaki Y *et al.* 2007 *Phys. Rev. B* **76** 184418
[5] Ivanov V Yu *et al.* 2006 *J. Magn. Magn. Mat.* **300** e130
[6] Danjoh S *et al.* 2009 *Phys. Rev.* B **80** 180408(R)
[7] Balbashov M *et al.* 1996 *J. Cryst. Growth* **67** 365
[8] Yaouanc A and Dalmas de Réotier P 2011 *Muon Spin Rotation, Relaxation, and Resonance* (Oxford: Oxford University Press)
[9] Kalvius G M, Noakes D R and Hartmann O 2001 in *Handbook on the Physics and Chemistry of Rare Earth* vol 32 chapter 206 (Amsterdam: Elsevier Science)
[10] Noakes D R 2002 *An Ornamental Garden of Field Distributions* http//musr.org/intro/ppt/GardenExport
[11] Kalvius G M *et al.* 2010 *J. Physics: Condens. Matter* **22** 052205
[12] Mostovoy M 2006 *Phys. Rev. Letters* **96** 067601
[13] Litterst F J *et al.* to be published
[14] Grandjean F and Long G J 1989 in *Mössbauer Spectroscopy Applied to Inorganic Chemistry* vol 3 (New York: Plenum press) p 513